Published in final edited form as:
J Mater Res. 2006 October ; 21(10): 2675–2682. doi:10.1557/JMR.2006.0334.

Synthesis of ultrasmooth nanostructured diamond films by microwave plasma chemical vapor deposition using a $He/H_2/CH_4/N_2$ gas mixture

S. Chowdhury, **Damon A. Hillman**, **Shane A. Catledge**, **Valery V. Konovalov**, and **Yogesh K. Vohra**[a]

Department of Physics, University of Alabama at Birmingham (UAB), Birmingham, Alabama 35294-1170; and UAB Center for Nanoscale Materials and Biointegration (CNMB), University of Alabama at Birmingham, Birmingham, Alabama 35294-1170

Abstract

Ultrasmooth nanostructured diamond (USND) films were synthesized on Ti–6Al–4V medical grade substrates by adding helium in $H_2/CH_4/N_2$ plasma and changing the N_2/CH_4 gas flow from 0 to 0.6. We were able to deposit diamond films as smooth as 6 nm (root-mean-square), as measured by an atomic force microscopy (AFM) scan area of 2 μm^2. Grain size was 4–5 nm at 71% He in (H_2 + He) and N_2/CH_4 gas flow ratio of 0.4 without deteriorating the hardness (~50–60 GPa). The characterization of the films was performed with AFM, scanning electron microscopy, x-ray diffraction (XRD), Raman spectroscopy, and nanoindentation techniques. XRD and Raman results showed the nanocrystalline nature of the diamond films. The plasma species during deposition were monitored by optical emission spectroscopy. With increasing N_2/CH_4 feedgas ratio (CH_4 was fixed) in $He/H_2/CH_4/N_2$ plasma, a substantial increase of CN radical (normalized by Balmer H_α line) was observed along with a drop in surface roughness up to a critical N_2/CH_4 ratio of 0.4. The CN radical concentration in the plasma was thus correlated to the formation of ultrasmooth nanostructured diamond films.

I. INTRODUCTION

In the United States, the need for long service life medical implants such as artificial joints is increasing rapidly. Wear of articulating surfaces is a major concern in orthopedic and dental implant devices, including the temporo-mandibular joint (TMJ), which resides in very close proximity to the eye, the ear, various nerves, and the brain.[1,2] The National Institute of Dental and Craniofacial Research (NIDCR) of the National Institutes of Health (NIH) states that over 10 million people in the United States suffer from TMJ problems at any given time.[3] In some cases, TMJ implant devices are needed, and their success is greatly influenced by the degree of wear at articulating surfaces. Complications arising from wear include component loosening, deleterious biological responses, osteolysis, mechanical instability, decreased joint mobility, increased pain, and ultimately implant failure.[4] A major goal is to develop smooth and wear-resistant films on the articulation surfaces to reduce the friction and wear in mating total joint replacement components. Hard, ultrasmooth, and wear resistance diamond films on metal surface can serve this purpose very well.

Chemical vapor deposited (CVD) diamond films grown using gas mixtures such as hydrogen, nitrogen, and methane have been investigated primarily to obtain smooth nanocrystalline

[a]Address all correspondence to this author. e-mail: ykvohra@uab.edu.

diamond film.[5–8] The surface roughness value of 15–20 nm (root-mean square; rms) and grain size of 13–15 nm were achieved. The film grown without nitrogen addition shows large, well-defined crystalline facets indicative of high-phase-purity diamond.[9] In contrast, the films grown with added nitrogen exhibit a nanocrystalline appearance with weak agglomeration into rounded nodules of submicron size. It has also been observed that the transformation from microcrystalline to nanocrystalline diamond structure can occur by adding Ar in H_2/CH_4 feed gases with a total transformation observed at Ar/H_2 volume ratio of 9.[10,11] Surface roughness as low as 18 nm and grain size of 3–50 nm were demonstrated on highly polished (area rms ~1 nm) silicon (111) wafers.[10] We have recently reported the effect of helium addition to $H_2/CH_4/N_2$ feedgas mixtures on growth of high-quality ultrasmooth nanostructured diamond films on Ti–6Al–4V.[12] The addition of He significantly reduced film roughness to 9–10 nm and grain size of diamond nanocrystals to 5–6 nm without deterioration of film hardness or adhesive properties.[12] In this article, we describe the synthesis of ultrasmooth nanostructured diamond films by using $He/H_2/CH_4/N_2$ plasma with different N_2/CH_4 volume ratio (CH_4 is fixed) in a microwave plasma chemical vapor deposition (MPCVD) reactor. Structural and mechanical properties were evaluated by x-ray diffraction (XRD), Raman spectroscopy, atomic force microscopy (AFM), scanning electron microscopy (SEM), and nanoindentation techniques.

II. EXPERIMENTAL DETAILS

Ti–6Al–4V alloy disks with 25.4 mm diameter and 3.4 mm thickness were punched from Ti–6Al–4V sheets supplied by Robin Materials (Mountain View, CA). They were polished to a rms roughness of 3–4 nm using a mechanical polisher with SiC paper, followed by a chemical–mechanical polish with a 0.06-μm colloidal silica solution containing 10% hydrogen peroxide. The polished disks were cleaned by ultrasonic agitation in a 1-μm diamond powder/water solution after a series of detergent solution, methanol, acetone, and finally, deionized water. Cleaned substrates were placed in a Wave-mat MPCVD reactor (Plymouth, MI), equipped with a 6 kW, 2.4 GHz microwave generator, as shown in Fig. 1. Chamber pressure was 65 Torr, and the substrate temperature, as measured by a Mikron M77LS Infraducer two-color infrared (IR) pyrometer, (Oakland, NJ) was kept in the range 690–720 °C by adjusting microwave power in the range 0.93–1.1 kW. This two-color pyrometer provided accurate measurement of the substrate temperature without requiring correction of the emissivity of the surface during growth. Total flow rate of He, H_2, and CH_4 gases was fixed at 336 sccm (71% He in He + H_2, 36 sccm of CH_4), and the ratio of N_2/CH_4 gas flow changed from 0 to 0.6.

Optical emission spectroscopy (OES) was performed to qualitatively determine the activated species present in the plasma. All the measurements were taken with 3000 points in the range of 350–700 nm wavelength and integration time of 250 ms. The crystallinity of the diamond films was analyzed by micro-Raman spectroscopy. The Raman spectra were taken using the 514.5 nm line of an argonion laser focused onto the film at a laser power of 100 mW. The Raman scattered signal was analyzed by a high-resolution spectrometer (1 cm^{-1} resolution) coupled to a charge-coupled device (CCD) system. XRD patterns on the diamond sample were examined using glancing angle XRD (X'pert MPD, Philips, Eindhoven, The Netherlands). XRD was performed using a glancing angle of 3° incident beam directed at the topmost surface of the coating surface. Spectra were taken from 30 to 90 (2θ) at a scan speed of 0.012° min^{-1} and a step size of 0.005°, as well as from 40 to 47 (2θ) to clearly document the intensity and full width at half-maximum (FWHM) of the diamond (111) diffraction peak.

Structure and surface morphology of the diamond surfaces was imaged by a TopoMetrix Explorer AFM (Santa Clara, CA). The images were collected in non-contact imaging mode. The cantilevers used were high resonance frequency (HRF) silicon I-shaped cantilevers with a frequency range of 279–318 kHz. The images obtained were processed by TopoMetrix SPM

Lab NT Version 5.0 software supplied with the microscope. The processing consists of a second order leveling of the surface and a left shading of the image. Roughness was measured from a 2 μm^2 scan area consistently for all samples. Surfaces of the diamond film were also imaged by FEI Nova NanoSEM (Hillsboro, OR).

The hardness and elastic modulus of the diamond films was measured using a Nanoindenter XP (MTS Systems, Oak Ridge, TN) system with a continuous stiffness attachment such that the loading and unloading displacement rates were constant. This provided continuous hardness/modulus measurements with increasing depth into the film.[13,14] The system was calibrated using silica samples for a range of operating conditions. Silica modulus and hardness were calculated as 70 GPa and 9.1 GPa and 69.6 and 9.4, respectively, before and after indentation on diamond samples. The tip functions before and after the indentation were held constant. A Berkovich diamond indenter with total included angle of 142.3° was used, and the maximum indentation depth of 150 nm was maintained for all the measurements. The data were processed using proprietary software to produce load–displacement curves, and the mechanical properties were calculated using the Oliver and Pharr method.[15]

III. RESULTS AND DISCUSSION

Previously, it was found that with the introduction of helium gas in $H_2/CH_4/N_2$ plasma, the transformation from microcrystalline to nanocrystalline occurred, and roughness decreased dramatically.[12] The roughness decreased from 19–20 nm to 9–10 nm with the introduction of helium up to 71% (in He/H_2 with fixed N_2 and CH_4 ratio 0.1). Helium gas was also introduced in H_2/CH_4 feedgas without N_2, and interestingly it was found that the roughness and grain size of the diamond films also decreased with increase of helium flow rate. The rms roughness was as low as 20 nm, and grain size was 16–18 nm at helium flow up to 71% (in He/H_2 with fixed CH_4 content), as shown in Figs. 2(a) and 2(b). It was found that the combined effect of He and N_2 played the vital role of decreasing the roughness and grain size and producing ultrasmooth nanocrystalline diamond films.[12] In this previous study, N_2/CH_4 ratio was fixed at 0.1, and the role of varying nitrogen on structure and morphology of diamond films was not investigated. In this study, we determined the effect of N_2 (N_2/CH_4 ratios 0.05–0.6) with fixed He, CH_4, and H_2 feedgases. There is a substantial difference between our growth chemistry and the chemistry used by the researchers from Argonne National Laboratory, Argonne, IL.[10,11,16] We have introduced much higher CH_4 feedgas (over 10%) compared to that typically used in the Argonne group (1%). Helium was introduced as a noble gas in our growth recipes, replacing argon. We used nitrogen feedgas addition, which is critical for achieving the smoothest nanophase diamond films. The Argonne group does not require nitrogen in their feedgas to produce their smooth diamond films which are characterized as “phase pure” nanocrystalline diamond. However, they have used nitrogen for doping, thus creating field-emission properties.[17]

According to Afzal et al.,[7] higher levels of gas phase CN radicals reduce the CH_3 concentration and thus reduce growth rate. Figure 3 shows the drop of the growth rate from 0.37 to 0.22 μm/h by changing N_2/CH_4 ratios from 0.05 to 0.6. In the inset of Fig. 3, an optical interference pattern collected from the interferometer is shown for the film deposited at N_2/CH_4 of 0.4. Optical emission spectroscopy was used to monitor the changes in plasma chemistry upon N_2 addition during diamond growth. The optical emission spectra of the $He/H_2/CH_4/N_2$ microwave plasmas with N_2/CH_4 ratios of 0.05 and 0.4 are shown in Fig. 4. The ratios of OES intensities of plasma species (CN/H_α, C_2/H_α and H_β/H_α) as a function of N_2/CH_4 ratio are also shown in Fig. 5. It was found that upon an increase of N_2/CH_4 ratio, the H_β/H_α remained practically constant, indicating only minor changes in plasma temperature. The ratio C_2/H_α remained almost constant, as well. Interestingly, the CN/H_α ratio increased from 1 to 5 up to the N_2/CH_4 ratio of 0.4 and then decreased afterwards. Previous results indicated that with an

increase of He addition up to 71% (in He + H_2) and N_2/CH_4 gas concentration ratio of 0.1, there was a 3-fold increase of CN/H_α.[12] With the same 71% of He (in He + H_2 gas mixture) addition but N_2/CH_4 gas concentration ratio of 0.4, we had increase of CN/H_α of 2.5 times. It decreased beyond a N_2/CH_4 ratio of 0.4.

Figure 6 shows the glancing angle XRD patterns for the nanostructured diamond films grown on Ti–6Al–4V alloy using the $He/CH_4/H_2/N_2$ feedgas mixture with different N_2/CH_4 ratios. Characteristic of these patterns are the cubic diamond (111) and (220) reflections as well as several peaks attributed to interfacial titanium carbide phases. The diamond peaks (shown in the inset) were significantly broadened as compared to those obtained from the conventional CVD process. The average grain size as calculated from the diamond (111) peak width using the Scherrer formula was between 4 and 8 nm. The grain size decreased to around 4–5 nm as N_2/CH_4 ratio increased up to 0.4 and then increased again. It was also found that as the N_2 content increased, the intensity of the (200) diffraction peak from the TiC phase decreased. At N_2/CH_4 of 0.4, there was no TiC peak, and the intensity again increased as the ratio N_2/CH_4 increased. The average grain size of diamond films with different N_2/CH_4 concentration ratios was estimated from the FWHM of the (111) diamond peak using the Scherrer equation (after correction for instrumental broadening) and is presented in Fig. 7. A SEM image at 300,000× on the surface of diamond sample grown in $He/H_2/CH_4/N_2$ plasma at N_2/CH_4 ratio of 0.4 is shown in Fig. 8. The grain size is as low as 5.7 nm and confirms the diamond nanostructure.

The micro-Raman spectra for each of the nanostructured diamond films on Ti–6Al–4V alloy are shown in Fig. 9. The diamond band at 1332 cm^{-1} is significantly broadened, and Raman scattering intensity in the 1400–1600 cm^{-1} region is pronounced. This band is usually associated with the “G-band” of disordered graphite which is downshifted from 1580 cm^{-1} and therefore likely involves scattering from amorphous sp^2 and sp^3 bonded carbon domains.[18] The Raman spectra have another peak at 1150 cm^{-1} in addition to the main diamond and graphite bands. It is suggested that this band is due to the nanocrystalline nature of the diamond films.[19] The films produced consist of diamond nanocrystallites imbedded in amorphous carbon matrix with a relatively small amount of graphitic carbon.

The plan-view AFM images in Fig. 10 of the as-grown diamond films show the morphological change due to change in different deposition conditions. Roughness measurements by AFM in the 2-μm^2 scan area for diamond films deposited in CH_4/H_2 plasma without N_2 [Fig. 10(a)] and with N_2 addition [Fig. 10(b)] were found to be 41 and 17 nm, respectively. The AFM images of diamond films with different N_2/CH_4 ratios in $He/H_2/CH_4/N_2$ plasma are shown in Figs. 10(c)–10(h). We could clearly observe the morphological change with change in the N_2 concentration in the feed gases. Earlier roughness measurement showed that by adding He in CH_4/H_2 feedgas (with no N_2) changed the roughness of the diamond films dramatically [shown in Fig. 2(b)]. We also reported 9–10-nm rms roughness value from diamond films deposited in $He/H_2/CH_4/N_2$ with 71% He in He + H_2 and a N_2/CH_4 ratio of 0.1.[12] When the N_2/CH_4 ratio was increased to 0.4 in the same gas mixture, roughness decreased even further to 6 nm (rms) and produced ultrasmooth diamond surfaces. These roughness values increased again with the increase of N_2/CH_4 ratios, as shown in Fig. 11. The nanoindentation load–displacement curve and hardness values for N_2/CH_4 ratio of 0.4 are given in Fig. 12. Nanoindentation measurement revealed that the hardness (H) and modulus (E) of diamond films with different N_2/CH_4 ratios were in the range of H = 50 to 60 GPa and E = 330 to 380 GPa, respectively.

The effect of He addition is not a simple effect of plasma dilution but is based on a more complex mechanism. Diamond films grown in $H_2/CH_4/N_2$ plasma without He at a corresponding high CH_4/H_2 ratio of 0.6 produced poor-quality films with a high content of the graphitic phase.[20] Helium addition reduced the diamond grain size, and this suggests that the

rate of secondary nucleation/renucleation increases in $He/H_2/CH_4/N_2$ plasma, terminating the growth of large diamond nanocrystals.[12] The effect of He addition was simply to increase the effective CH_4/H_2 ratio in $He/H_2/CH_4/N_2$ plasma, which should reduce the effect of hydrogen on suppressing secondary nucleation by regasifying nondiamond carbon. Helium has also a strong influence on the CN radical on the degree of diamond nanocrystallinity.[6–8] Small amounts of CN and HCN in conventional mixtures (CH_4/H_2) effectively abstract adsorbed H atoms, creating vacant growth sites, thereby reducing the carbon supersaturation.[21–23] The use of large N_2 additions (N_2/CH_4 ratios greater than 0.05) resulted in a reduction of diamond phase purity, a more nanocrystalline structure, and a smoother film surface. The larger amounts of CN and HCN resulted in excessive abstraction of adsorbed H, which leaves the surface open to further adsorption by CN or other nitrogen species that are not able to stabilize the diamond structure efficiently.[23] Therefore, higher CN species promote higher nanocrystallinity and more CN species form in N_2 and He gas mixture. Apart from causing the nanocrystallinity of the diamond component in the film, the addition of nitrogen in the gas phase also resulted in amorphous carbon content in the film with a corresponding increase in the Raman 1550 cm^{-1} peak intensity.[24] Higher CN levels also induced increased twinning, and stacking faults resulting in the nanocrystalline structure.[7] Our previous OES measurements taken from He/$He/CH_4/N_2$ plasma reflected that, at 71% He content and N_2/CH_4 ratio of 0.1, both the CN/H_α and C_2/H_α were maximized. The present results indicated that at the same 71% He content and 0.4 N_2/CH_4 gas flow ratio there was an increase of 2.5 the CN/H_α ratio. There was no significant change in C_2/H_α values. The lowest roughness and smaller grain size values were achieved in the diamond films at the N_2/CH_4 ratio of 0.4. Thus, CN has a strong influence on the formation of smooth nanocrystalline diamond films, and the activity of CN radical is highly affected by the addition of He.

IV. CONCLUSION

In summary, we have synthesized ultrasmooth nanostructured diamond films on Ti–6Al–4V medical grade substrates by adding helium in $H_2/CH_4/N_2$ plasma and by changing the N_2/CH_4 gas flow from 0 to 0.6. We were able to deposit diamond films with 6 nm (rms) roughness in 2 μm^2 area and grain size of 4–5 nm. Roughness decreased from rms 22 to 6 nm from N_2/CH_4 gas flow ratio of 0.05 to 0.4 (CH_4 is fixed) and then increased again up to 13 nm at N_2/CH_4 ratio of 0.6. Raman spectra were typical for nanostructured diamond films and did not show significant changes with varying N_2/CH_4 ratio. Nanoindentation demonstrated that the hardness and Young's modulus of the films are in the range of 50–60 GPa and 330–380 GPa, respectively. X-ray diffraction showed that all the spectra have broad diamond (111) peaks characteristic of nanostructure diamond, and the grain size was calculated between 4 and 8 nm. The grain size decreased and drop to around 4–5 nm as the N_2/CH_4 ratio increased up to 0.4 and then again increased. The surface morphology imaged by nano SEM at 300,000× also confirmed the nanocrystalinity of the diamond films. It was also found that as the N_2 content increased, the intensity of the TiC peak decreased. At a N_2/CH_4 ratio of 0.4, there was no (200) TiC peak, and the intensity again increased as the N_2/CH_4 ratio increased beyond 0.4. It was previously described that reducing diamond grain size and film surface roughness by He addition is attributed to plasma dilution, enhanced fragmentation of carbon containing species, and enhanced formation of CN radical. From optical emission data, we found that CN/H_α relative intensity was highest at a N_2/CH_4 gas concentration ratio of 0.4, which resulted in the smoothest nanostructured hard diamond films. Therefore, it can be concluded that CN radical has a strong influence in formation of smooth nanocrystalline diamond films.

Acknowledgements

We acknowledge support from the National Institute of Dental and Craniofacial Research (NIDCR), National Institutes of Health (NIH) under Grant No. R01 DE013952.

References

1. Saha S, Campbell C, Sarma A, Christiansen R. A biomechanical evaluation of the christensen temporomandibular joint implant. Crit Rev Biomed Eng 2000;28:399. [PubMed: 11108206]
2. Shankland, WE. TMJ: Its Many Faces. 2. Anadem Publishing; Columbus, OH: 1998. p. 15
3. National Center for Health Statistics. Vital Health Statistics, 1994 Report. Hyattsville, MD: 1994.
4. Praemer, S.; Furner, D. Musculoskeletal conditions in the United States. AAOS; Rosemont, IL: 1992. p. 125
5. Catledge SA, Vohra YK. High-density plasma processing of nanostructured diamond films on metals. J Appl Phys 1998;84:6469.
6. Catledge SA, Borham J, Vohra YK, Lacefield WR, Lemons JE. Nanoindentation hardness and adhesion investigations of vapor deposited nanostructured diamond films. J Appl Phys 2002;91:5347.
7. Afzal A, Rego CA, Ahmed W, Cherry RI. HFCVD diamond grown with added nitrogen: Film characterization and gas-phase composition studies. Diamond Relat Mater 1998;7:1033.
8. Corvin RB, Harrison JG, Catledge SA, Vohra YK. Gas-phase thermodynamic models of nitrogen-induced nanocrystallinity in chemical vapor-deposited diamond. Appl Phys Lett 2002;80:2550.
9. Catledge SA, Vohra YK. Mechanical properties and quality of diamond films synthesized on Ti–6Al–4V alloy using the microwave plasmas of CH_4/H_2 and CO/H_2 systems. J Appl Phys 1998;83:198.
10. Zhou D, Gruen DM, Qin LC, McCauley TG, Krauss AR. Control of diamond film microstructure by Ar additions to CH_4/H_2 microwave plasmas. J Appl Phys 1998;84:1981.
11. Gruen DM. Nanocrystalline diamond films. Ann Rev Mater Sci 1999;29:211.
12. Konovalov VV, Melo A, Catledge SA, Chowdhury S, Vohra YK. Ultra-smooth nanostructured diamond films deposited from $He/H_2/CH_4/N_2$ microwave plasmas. J Nanosci Nano-technol 2006;6:258.
13. Fabes BD, Oliver WC, McKee RA, Walker FJ. The determination of film hardness from the composite response of film and substrate to nanometer scale indentations. J Mater Res 1992;7:3056.
14. McHargue, J. Mechanical properties and applications of diamond. In: Tzeng, Y.; Yoshikawa, M.; Murakawa, M.; Feldman, A., editors. Applications of Diamond Films and Related Materials. Elsevier; Amsterdam, The Netherlands: 1991. p. 113
15. Oliver WC, Pharr GM. An improved technique for determining hardness and elastic modulus using load and displacement sensing indentation experiments. J Mater Res 1992;7:1564.
16. Zhou D, McCauley TG, Qin LC, Krauss AR, Gruen DM. Synthesis of nanocrystalline diamond thin films from an $Ar–CH_4$ microwave plasma. J Appl Phys 1997;83:540.
17. Zhou D, Krauss AR, Qin LC, McCauley TG, Gruen DM, Corrigan TD, Chang RPH, Gnaser H. Synthesis and electron field emission of nanocrystalline diamond thin films grown from N_2/CH_4 microwave plasmas. J Appl Phys 1997;82:4546.
18. Tamor MA, Vassell WC. Raman “fingerprinting” of amorphous carbon films. J Appl Phys 1994;76:3823.
19. Nemanich J, Glass JT, Lucovsky G, Shroder RE. Raman scattering characterization of carbon bonding in diamond and diamondlike thin films. J Vac Sci Technol A 1988;6:1783.
20. Catledge, SA.; Vohra, YK. Mechanical Properties of Structural Films. ASTM STP1413, ASTM; West Conshohocken, PA: 2001. Effect of nitrogen feedgas addition on the mechanical properties of nano-structured carbon coatings; p. 5
21. Jin S, Moustakas TD. Effect of nitrogen on the growth of diamond films. Appl Phys Lett 1994;65:403.
22. Cao GZ, Schermer JJ, van Enckevort WJP, Elst WALM, Giling LJ. Growth of {100} textured diamond films by the addition of nitrogen. J Appl Phys 1996;79:1357.
23. Bohr S, Haubner R, Lux B. Influence of nitrogen additions on hot-filament chemical vapor deposition of diamond. Appl Phys Lett 1996;68:1075.
24. Catledge SA, Vohra YK. Effect of nitrogen addition on the microstructure and mechanical properties of diamond films grown using high-methane concentrations. J Appl Phys 1999;86:698.

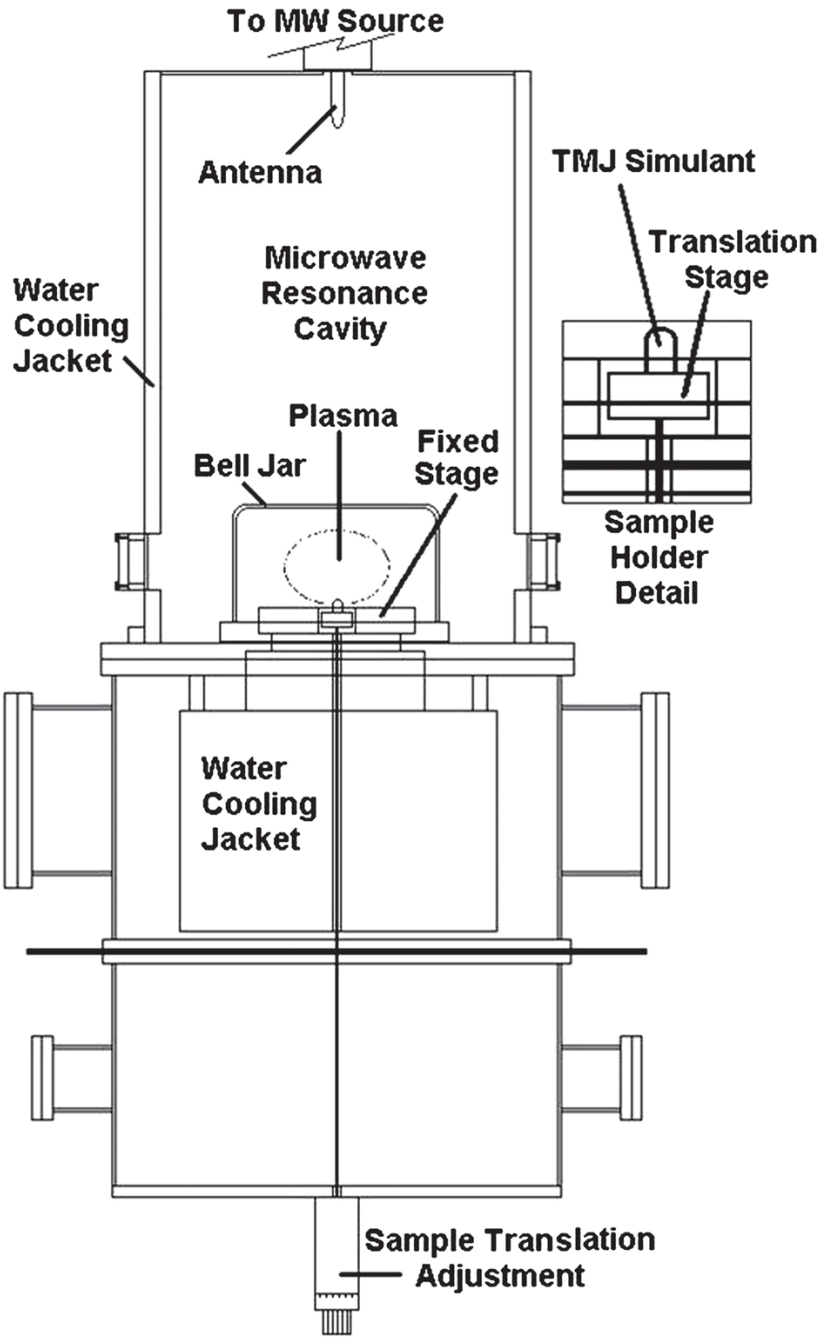

FIG. 1.
Schematic illustration of the MPCVD reactor.

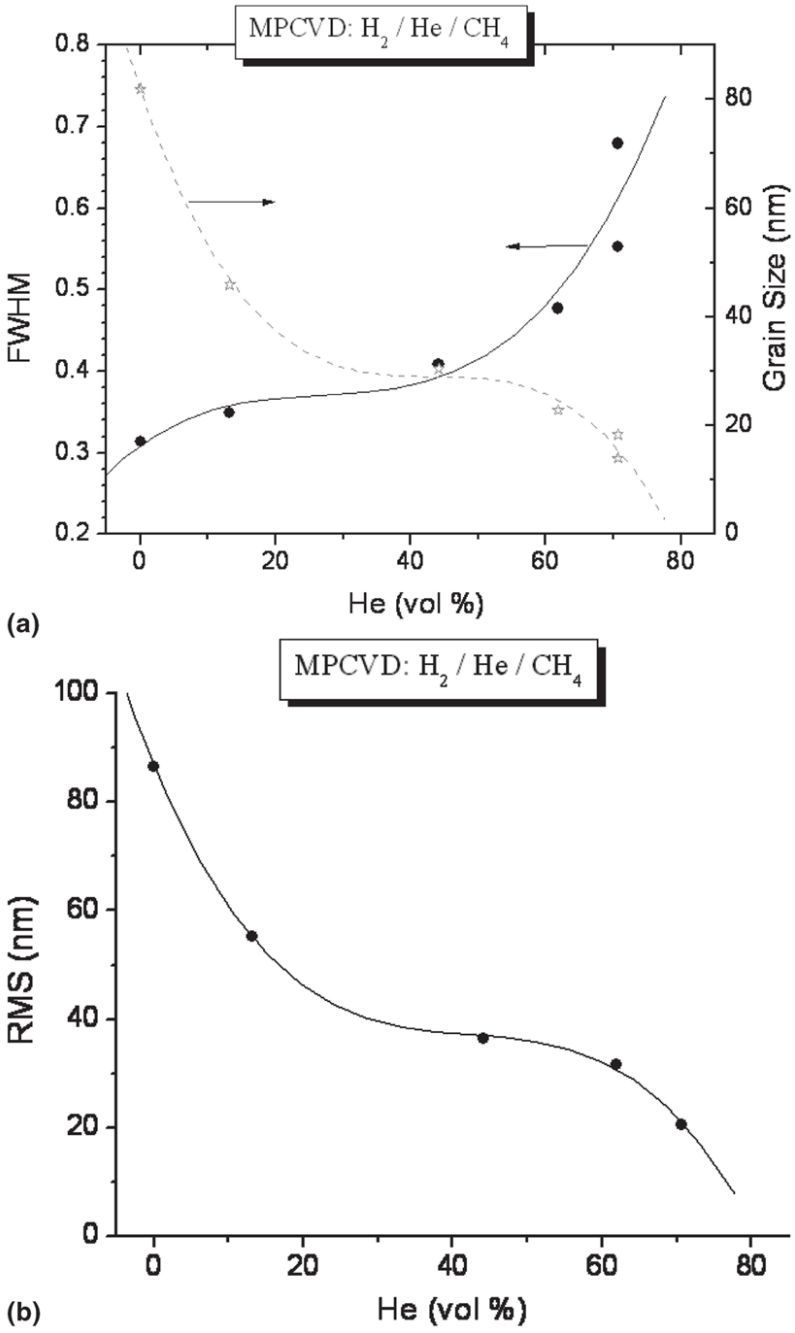

FIG. 2.

Diamond films grown in $He/H_2/CH_4$ plasma at different He contents and no N_2: (a) FWHM of the (111) diamond XRD peak and calculated average diamond grain size and (b) rms surface roughness of the films calculated from 2 × 2 μm AFM images.

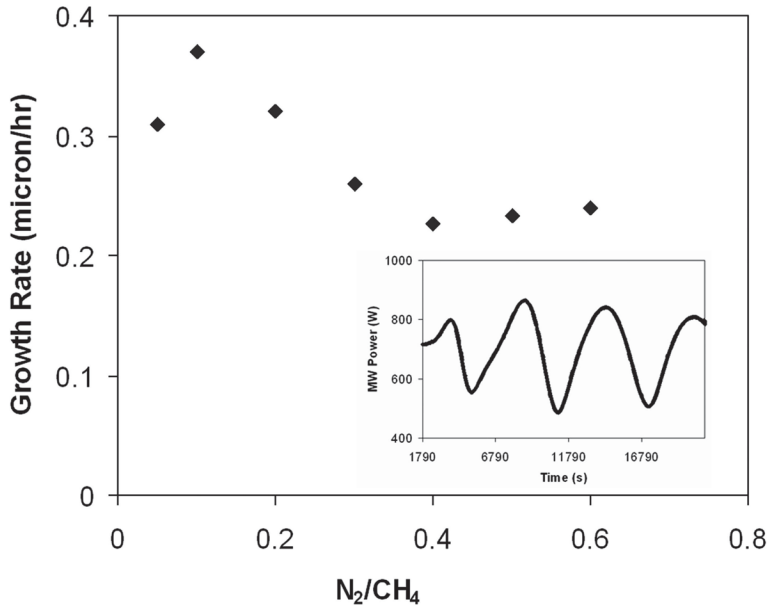

FIG. 3.

Growth rate of diamond films at different N_2/CH_4 volume ratio in $He/H_2/CH_4/N_2$ plasma. In the inset, the optical interference pattern collected from interferometer is shown for film deposited at $N_2/CH_4 = 0.4$.

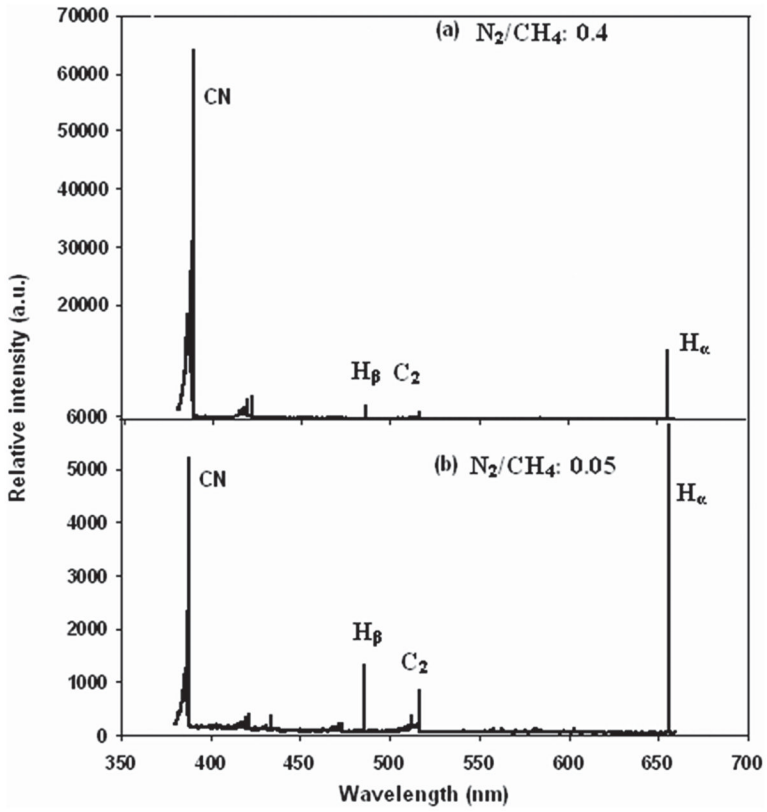

FIG. 4.

Optical emission spectra of the $He/H_2/CH_4/N_2$ microwave plasmas with different ratios of N_2/CH_4: (a) $N_2/CH_4 = 0.4$ and (b) $N_2/CH_4 = 0.05$. It is to be noted that the intensity scales in the two spectra are different; CN peaks increase in intensity by a factor of ten in (a).

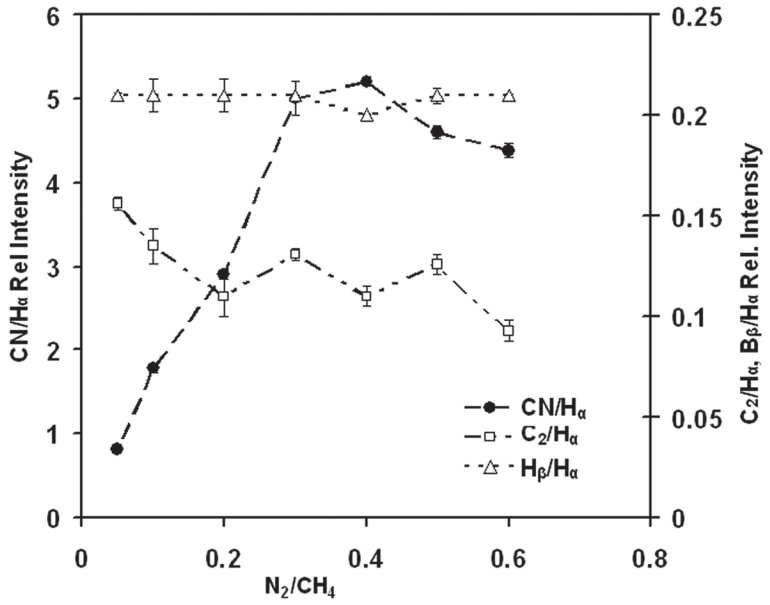

FIG. 5.

Normalized optical emission intensities of Balmer H_β (486.14 nm), C_2 (516.5 nm), and CN (386 nm) lines versus N_2/CH_4 content in $He/H_2/CH_4/N_2$ plasma. Lines were normalized to Balmer H_α line (656.3 nm) intensity.

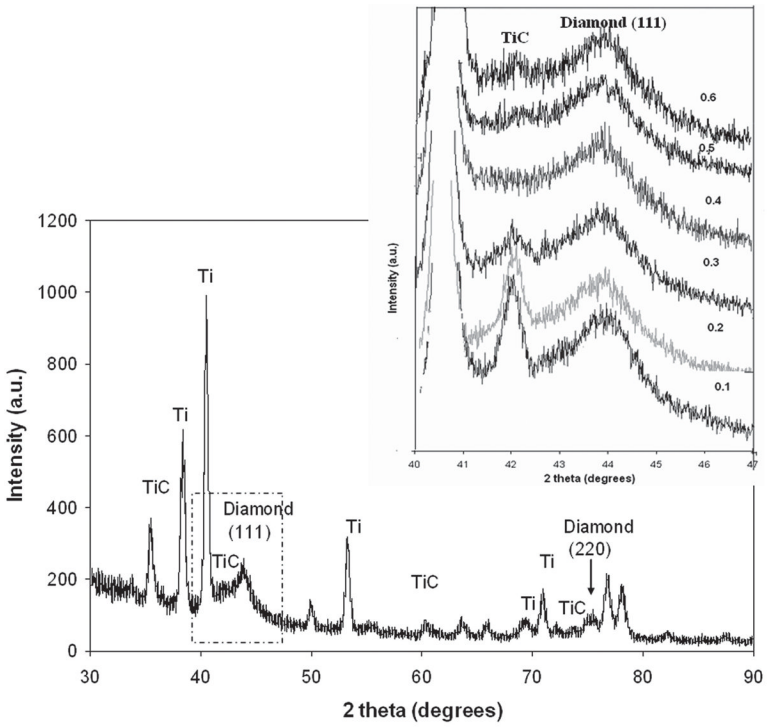

FIG. 6.

X-ray diffraction patterns of the $He/H_2/CH_4/N_2$ microwave plasmas with different ratio of N_2/CH_4. The inset shows the close-up view of TiC and diamond (111) peaks showing the change due to the change of N_2/CH_4 volume ratio.

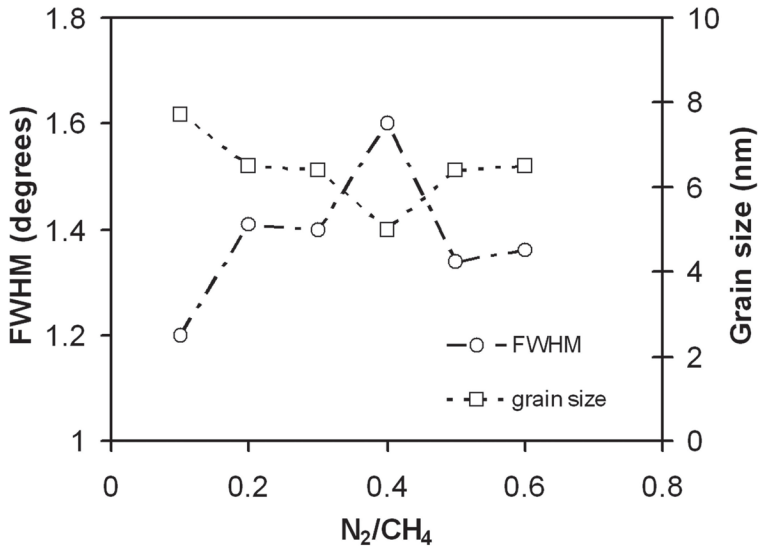

FIG. 7.

FWHM of the diamond (111) XRD peak and calculated average diamond grain size of diamond films grown in $He/H_2/CH_4/N_2$ plasma at different N_2/CH_4 flow ratio.

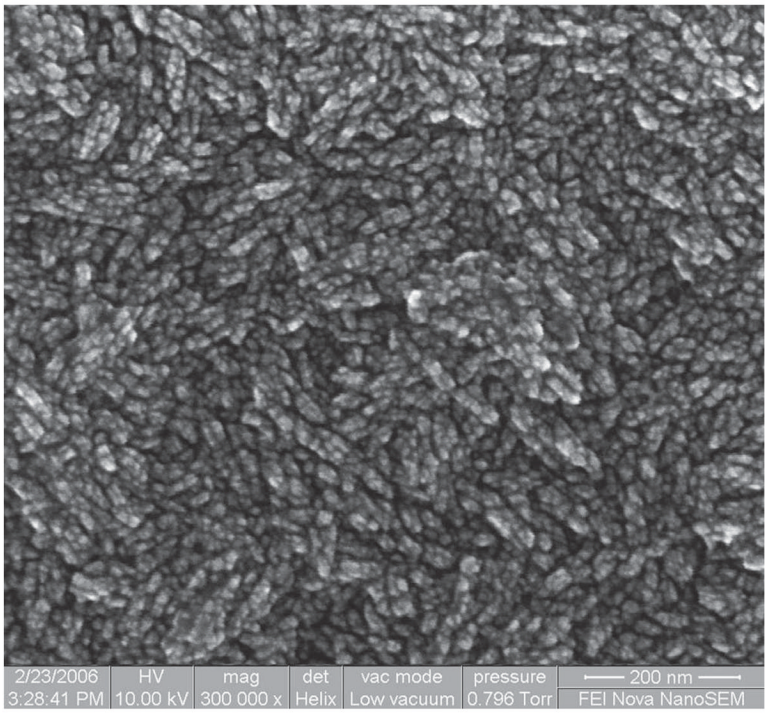

FIG. 8.

SEM image at 300,000× of the diamond film surface grown in $He/H_2/CH_4/N_2$ plasma at N_2/CH_4 flow ratio of 0.4.

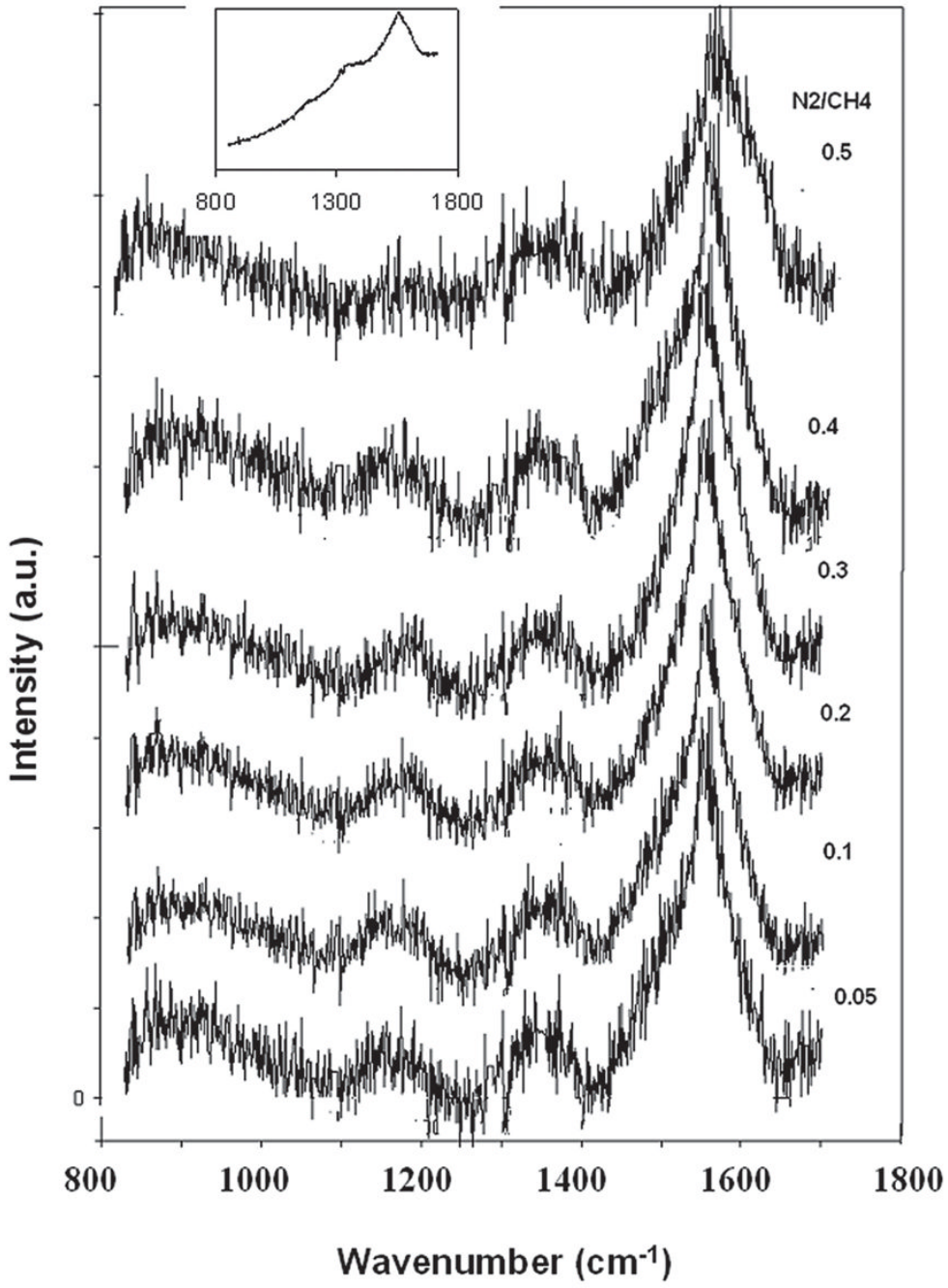

FIG. 9.

Micro-Raman spectra for high-density plasma processed nanostructured diamond films on Ti–6Al–4V alloy at different N_2/CH_4 feed gas fractions. The spectra were background subtracted from the as-received one shown in the inset and are displaced along vertical axis for visual clarity.

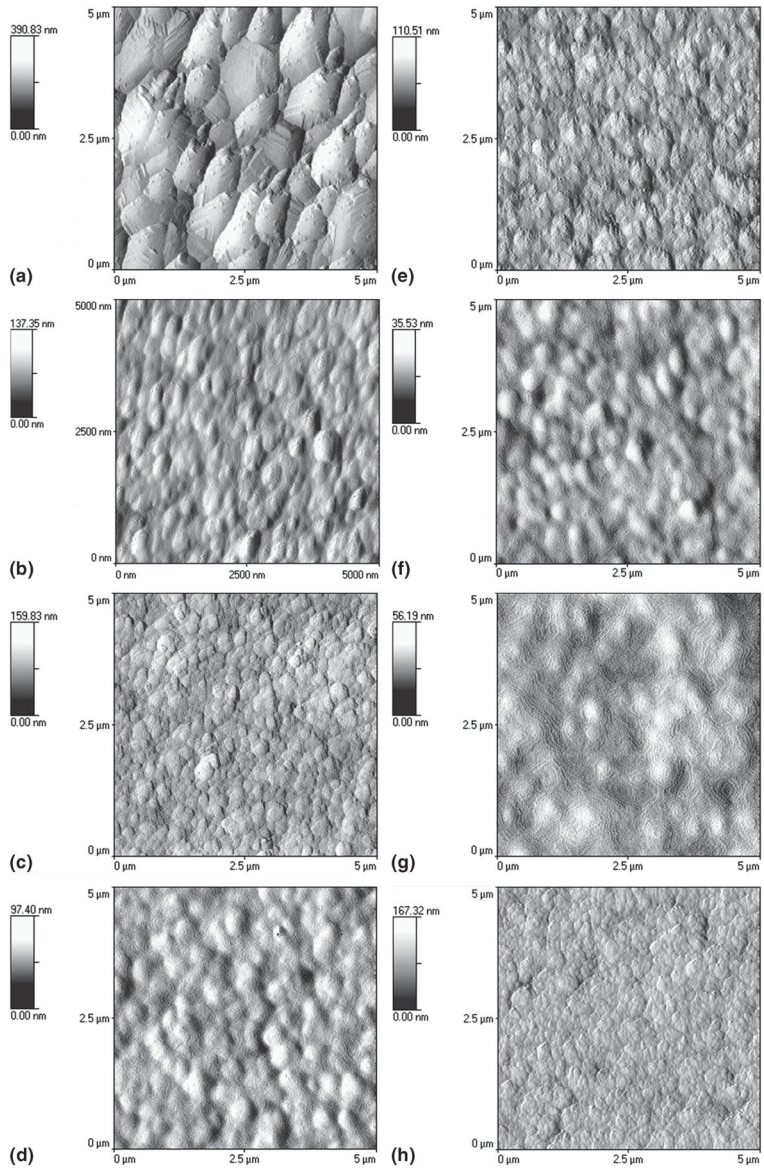

FIG. 10.

Plan-view AFM images of the as-grown diamond films prepared from microwave plasma showing the morphological change due to change in different deposition conditions: (a) CH_4/H_2 plasma without N_2, (b) CH_4/H_2 plasma with N_2, (c–h) $He/H_2/CH_4/N_2$ plasma with different N_2/CH_4 ratios: N_2/CH_4 = (c) 0.05, (d) 0.1, (e) 0.2, (f) 0.3, (g) 0.4, and (h) 0.5.

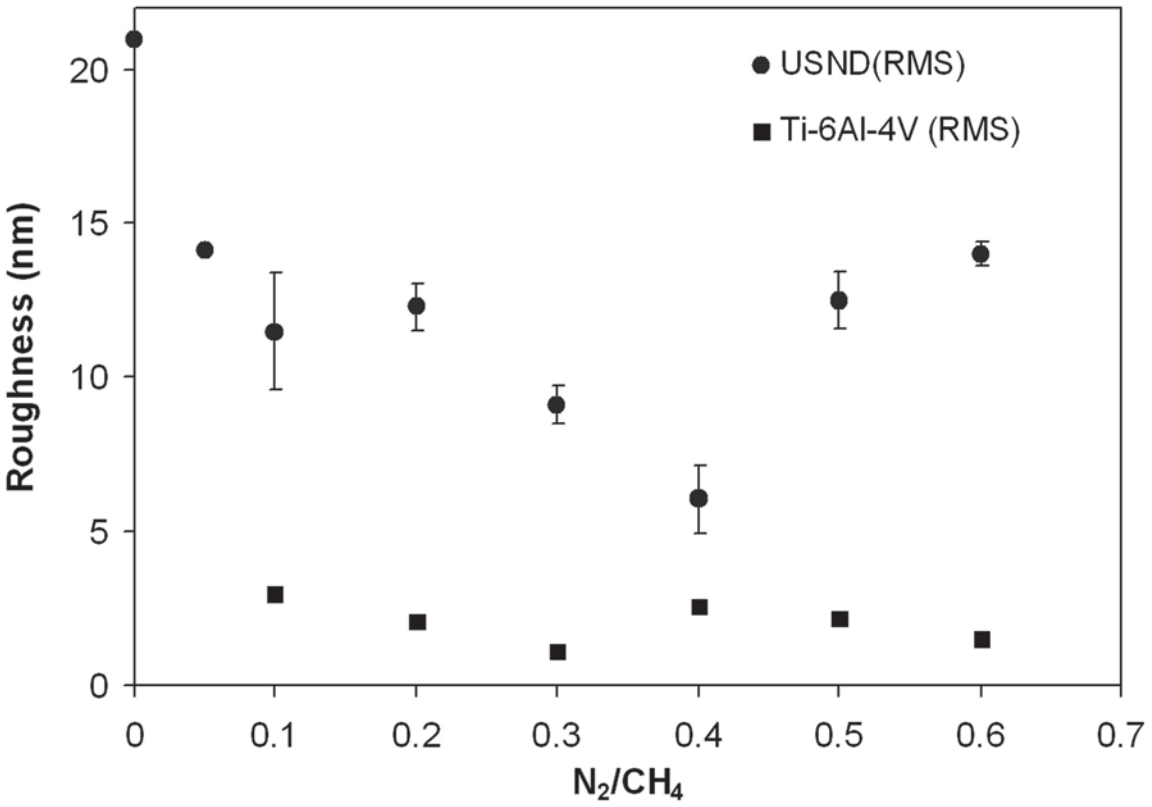

FIG. 11.

A plot of the surface roughness measured in 2 × 2 μm area of different as-grown diamond films with different N_2/CH_4 ratios in $He/H_2/CH_4/N_2$ plasma. Roughness values are also given for uncoated polished Ti-6Al-4V substrates.

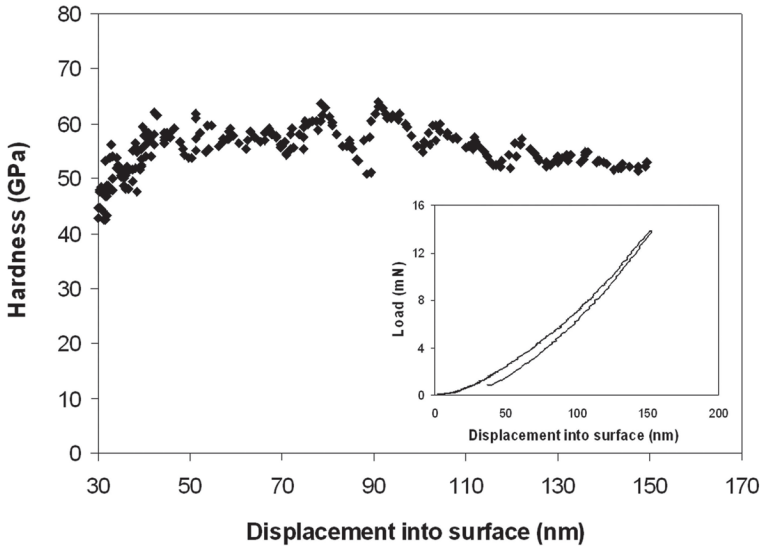

FIG. 12.

Nanoindentation hardness versus depth for high density plasma processed ultra smooth nanostructured diamond coating at N_2/CH_4 ratio 0.3 in $He/H_2/CH_4/N_2$ plasma. Nanoindentation load-displacement curve for same sample is shown in the inset.